Integration of a Reconstituted de Novo Synthesized Hemoprotein and Native Metalloproteins with Electrode Supports for Bioelectronic and Bioelectrocatalytic Applications

Itamar Willner,*,†,‡ Vered Heleg-Shabtai,† Eugenii Katz,† Harald K. Rau,§ and Wolfgang Haehnel*,§

Contribution from the Institute of Chemistry, The Hebrew University of Jerusalem, Jerusalem 91904, Israel, and Institut für Biologie II/Biochemie, Albert-Ludwigs-Universität Freiburg, Schänzlestrasse 1, D-79104 Freiburg, Germany

Received September 8, 1998. Revised Manuscript Received March 22, 1999

Abstract: A four-helix bundle de novo synthesized protein is assembled as a monolayer onto a Au electrode. Two of the helices include each two histidine units. This allows the reconstitution of the de novo protein with two Fe(III)−protoporphyrin IX units. Electrochemical characterization of the bis-heme-functionalized de novo protein, surface coverage 2.5×10^{-11} mol·cm^{-2}, reveals that the heme site close to the electrode surface exhibits a redox potential, $E^\circ = -0.43$ V (vs SCE), whereas the heme center in the remote position with respect to the electrode exhibits a more positive potential, $E^\circ = -0.36$ V (vs SCE). This enabled the use of the de novo protein as a rectifier element in which rapid vectorial electron transfer occurs. The bis-heme-functionalized de novo protein assembled onto the electrode forms an affinity complex with the cytochrome b_1-dependent nitrate reductase (NR, E.C. 1.9.6.1). The affinity complex was cross-linked with glutaric dialdehyde to yield an integrated, electrically contacted, enzyme electrode for the effective bioelectrocatalyzed reduction of NO_3^-, current yield 80%. Similarly, the bis-heme-reconstituted de novo protein assembly forms an affinity complex with Co(II)−protoporphyrin-reconstituted myoglobin, Co(II)−Mb. Cross-linking of the affinity complex between the de novo synthesized hemoprotein and Co(II)−Mb with glutaric dialdehyde results in an integrated bioelectrocatalytic electrode for the electrocatalyzed hydrogenation of acetylene dicarboxylic acid (**3**) to maleic acid (**4**), current yield 85%.

Introduction

Directionality of electron transfer is a basic feature of many biological processes, e.g., photosynthesis.[1] The organization of ordered redox-active protein arrays for vectorial electron transfer is still a challenging scientific topic.[2] One possible approach to tailor directional electron transfer in biomaterial assemblies involves the engineering of surfaces, e.g., electrodes, with redox-active components exhibiting an appropriate thermodynamic gradient for an electron-transfer cascade. For this purpose, it is, however, essential to design the electrical communication between the biomaterial and the electrode transducer. Electrical contacting of redox proteins and electrode surfaces is of fundamental interest in the application of redox-active biomaterials in bioelectronic devices such as biosensors,[3] biofuel cells,[4] and optobioelectronic systems.[5] The modification of redox enzymes with electroactive relay groups, or the immobilization of the biocatalysts in redox-functionalized polymers, provides means to establish electrical communication between the redox centers in the proteins and the electrode surfaces.[6] Recently, reconstitution of apo-flavoenzymes on a relay-FAD monolayer-functionalized electrode was reported to yield an aligned biocatalyst on an electrode support that exhibits effective electrical contact with the electrode surface.[7] This concept of tailoring integrated and aligned bioelectrocatalytic complexes

† The Hebrew University of Jerusalem.

‡ Phone: 972-2-6585272. Fax: 972-2-6527715. E-mail: willnea@vms.huji.ac.il.

§ Albert-Ludwigs-Universität Freiburg.

(1) (a) Deisenhofer, J.; Epp, O.; Miki, K.; Huber, R.; Michel, H. *Nature* **1985**, *318*, 618. (b) Isied, S. S.; Ogawa, M. J.; Wishart, J. W. *Chem. Rev.* **1992**, *92*, 381. (c) Winkler, J. R.; Gray, H. B. *Chem. Rev.* **1992**, *92*, 369. (d) Kartha, S.; Das, R.; Norris, J. R. In *Metal Ions in Biological Systems, Electron-Transfer Reactions in Metalloproteins*; Sigel, H., Sigel, A., Eds.; Marcel Dekker: New York, 1991; Vol. 27, Chapter 10, pp 323−360.

(2) (a) McLendon, G. *Acc. Chem. Res.* **1988**, *21*, 160. (b) Heleg-Shabtai, V.; Gabriel, T.; Willner, I. *J. Am. Chem. Soc.* **1999**, *121*, 3220. (c) Kostic, N. M. In *Metal Ions in Biological Systems, Electron-Transfer Reactions in Metalloproteins*; Sigel, H., Sigel, A., Eds.; Marcel Dekker: New York, 1991; Vol. 27, Chapter 4, pp 129−182.

(3) (a) Heller, A. *J. Phys. Chem.* **1992**, *96*, 3579. (b) Schmidt, H.-L.; Schuhmann, W. *Biosens. Bioelectron.* **1996**, *11*, 127. (c) Katz, E.; Heleg-Shabtai, V.; Willner, B.; Willner, I.; Bückmann, A. F. *Bioelectrochem. Bioenerg.* **1997**, *42*, 95. (d) Willner, I.; Katz, E.; Willner, B. *Electroanalysis* **1997**, *9*, 965. (e) Willner, I.; Katz, E.; Willner, B. In *Biosensors and Their Applications*; Yang, V. C., Ngo, T. T., Eds.; Plenum Press: New York, in press.

(4) (a) Willner, I.; Arad, G.; Katz, E. *Bioelectrochem. Bioenerg.* **1998**, *44*, 209. (b) Willner, I.; Katz, E.; Patolsky, F.; Bückmann, A. F. *J. Chem. Soc., Perkin Trans. 2* **1998**, 1817.

(5) (a) Katz. E.; Willner, B.; Willner, I. *Biosens. Bioelectron.* **1997**, *12*, 703. (b) Willner, I. *Acc. Chem. Res.* **1997**, *30*, 347. (c) Willner, I.; Lion-Dagan, M.; Marx-Tibbon, S.; Katz, E. *J. Am. Chem. Soc.* **1995**, *117*, 6581.

(6) (a) Degani, Y.; Heller, A. *J. Phys. Chem.* **1987**, *91*, 1285. (b) Degani, Y.; Heller, A. *J. Am. Chem. Soc.* **1988**, *110*, 2615. (c) Schuhmann, W.; Ohara, T. J.; Schmidt, H.-L.; Heller, A. *J. Am. Chem. Soc.* **1991**, *113*, 1394. (d) Bartlett, P. N.; Whitaker, R. G.; Green, M. J.; Frew, J. *J. Chem. Soc., Chem. Commun.* **1987**, 1603. (e) Badia, A.; Carlini, R.; Fernandez, A.; Battaglini, F.; Mikkelsen, S. R.; English, A. M. *J. Am. Chem. Soc.* **1993**, *115*, 7053. (f) Willner, I.; Katz, E.; Riklin, A.; Kasher, R. *J. Am. Chem. Soc.* **1992**, *114*, 10965. (g) Willner, I.; Lapidot, N.; Riklin, A.; Kasher, R.; Zahavy, E.; Katz, E. *J. Am. Chem. Soc.* **1994**, *116*, 1428. (h) Katz, E.; Riklin, A.; Willner, I. *J. Electroanal. Chem.* **1993**, *354*, 129. (i) Cosnier, S. *Electroanalysis* **1997**, *9*, 894. (j) Willner, I.; Willner, B. *React. Polym.* **1994**, *22*, 267.

10.1021/ja983182u CCC: $18.00
Published on Web 06/25/1999

was further broadened to organize enzyme electrodes by the cross-linking of cofactor−biocatalyst affinity complexes on the electrode surface. The resulting electrically contacted enzyme electrodes were then applied as biosensors.[8] Reconstitution of apo-proteins with semisynthetic or synthetic groups analogous to the native active site was recently employed as a means to engineer new functions of proteins. Reconstitution of apo-glucose oxidase or apo-amino acid oxidase with a ferrocene-tethered FAD cofactor generated redox enzymes exhibiting electrical communication with electrode surfaces.[9] Reconstitution of apo-myoglobin with Co(II)−protoporphyrin IX, and substitution of the protein with a chromophore, was reported to yield a "photoenzyme" where photoinduced electron transfer, followed by charge separation, enables the photocatalyzed hydrogenation of acetylenes, e.g., acetylenedicarboxylic acid to maleic acid.[10] Various enzymes, e.g., cytochrome oxidase or lactate dehydrogenase, were electrically contacted with electrodes via the formation of affinity complexes with the low molecular weight cytochrome *c* hemoprotein. Other redox proteins such as nitrate reductase or Co(II)−protoporphyrin IX-reconstituted myoglobin exhibited, however, electrical communication with electrodes only in the presence of heme-derivatized oligopeptides, e.g., microperoxidase-11.[8b,c]

Extensive research efforts are directed to the de novo synthesis of proteins that provide a methodology of wide variability in biomimetic chemistry.[11,12] In particular, the approach to prepare synthetic proteins by antiparallel α-helix elements on a cyclic peptide provides an efficient strategy for the synthesis of predetermined structures.[13] This method was successfully applied in tailoring a synthetic cytochrome *b* analogue by the assembly of four antiparallel helices containing two heme binding sites in the hydrophobic interior.[14] The elucidation of the catalytic properties and tailored redox functions of these synthetic proteins remains a challenging perspective in the future design of bioelectronic systems.

Here we report on the assembly of a four-helix-bundle synthetic protein as a monolayer on a Au electrode. We demonstrate the stepwise reconstitution of two Fe(III)−protoporphyrin IX complexes into the synthetic protein. We analyze the kinetics of electron transfer between the electrode and the synthetic hemoprotein, and identify a vectorial electron transfer in the assembly and the function of the system as a rectifier.[15] We also demonstrate that the synthetic hemoprotein monolayer acts as an electron-transfer mediator for native redox proteins, e.g., nitrate reductase, or a semisynthetic chemically engineered protein, i.e., Co(II)−protoporphyrin IX-reconstituted myoglobin. Mediated electron transfer from the synthetic de novo hemoprotein to the redox enzymes proceeds via the formation of affinity complexes between the components. By cross-linking the two-dimensional affinity complex arrays on the electrode support, integrated and stable electrically contacted enzyme electrodes for biosensor and bioelectrocatalytic applications are generated. Methods for assembling the functionalized electrodes are discussed, and means to regenerate the modified electrodes are addressed.

Experimental Section

Materials. The de novo protein was synthesized as described previously[14] from unprotected, HPLC-purified peptides by the reaction of bromoacetyl-*N*-lysine residues (of helix B) and bromoacetylglycine residues (of helix A) which were coupled to cysteine SH groups of the template. Co^{II}-derivatized myoglobin, Co^{II}−Mb, was prepared as previously described.[16] 2-Chloro-3-(3-carboxypropylamine)-1,4-naphthoquinone (**1**) was synthesized according to the published procedure.[17] All other chemicals, including *N*-succinimidyl-3-maleimidopropionate (**2**), cystamine (2,2′-diaminodiethyl disulfide), cysteamine (2-aminoethanethiol), glutaric dialdehyde, acetylenedicarboxylic acid (**3**), Fe(III)−protoporphyrin IX, 1-[(3-dimethylamino)propyl]-3-ethylcarbodiimide (EDC), 4-(2-hydroxyethyl)piperazine-1-ethanesulfonic acid sodium salt (HEPES), myoglobin (from horse heart), and nitrate reductase (cytochrome kind, E.C. 1.9.6.1, from *Escherichia coli*, 5 u g^{-1}) were used as supplied (Aldrich or Sigma). Ultrapure water Elgastat UHQ source was used throughout this work.

Electrode Modification. Au electrodes (0.5 mm diameter Au wire, geometrical area ca. 0.2 cm^2, roughness factor ca. 1.3) were cleaned as previously described.[18] In some specially indicated experiments, the electrode surface was roughened[19] by its amalgamation with mercury and further dissolution of the amalgam layer in HNO_3. This latter treatment results in a typical roughness factor of ca. 20−30. Rough Au electrodes of larger size (gold plate, geometrical area ca. 2 cm^2) were used in some measurements. A cyclic voltammogram recorded in 0.5 M H_2SO_4 was used to determine the purity of the electrode surface just before modification.[20] The real electrode surface area and roughness coefficient were estimated from the same cyclic voltammogram by integrating the cathodic peak for the electrochemical reduction of the oxide layer on the electrode surface. Smooth Au electrodes were used to characterize electrochemical properties of the immobilized de novo protein monolayer, and rough Au electrodes were applied to perform biocatalytic transformations at modified surfaces.

Primary electrode modification with cystamine was performed as described previously.[18,19] The cystamine-modified Au electrode was reacted with 1×10^{-3} M solution of *N*-succinimidyl-3-maleimidopropionate (**2**) in DMSO for 2 h, followed by rinsing with water. The maleimide-functionalized Au electrode was treated with the de novo protein, 0.5 mg mL^{-1}, in 0.1 M phosphate buffer, pH 7.0, for 2 h, followed by rinsing with water. The resulting de novo protein monolayer was reconstituted with two Fe(III) heme sites by its soaking in 1×10^{-3} M Fe(III)−protoporphyrin IX solution in DMSO for 2 h, followed

(7) (a) Willner, I.; Heleg-Shabtai, V.; Blonder, R.; Katz, E.; Tao, G.; Bückmann, A. F.; Heller, A. *J. Am. Chem. Soc.* **1996**, *118*, 10321. (b) Katz, E.; Riklin, A.; Heleg-Shabtai, V.; Willner, I.; Bückmann, A. F. *Anal. Chim. Acta* **1999**, *385*, 45.

(8) (a) Bardea, A.; Katz, E.; Bückmann, A. F.; Willner, I. *J. Am. Chem. Soc.* **1997**, *119*, 9114. (b) Heleg-Shabtai, V.; Katz, E.; Willner, I. *J. Am. Chem. Soc.* **1997**, *119*, 8121. (c) Heleg-Shabtai, V.; Katz, E.; Levi, S.; Willner, I. *J. Chem. Soc., Perkin Trans. 2* **1997**, 2645. (d) Patolsky, F.; Katz, E.; Heleg-Shabtai, V.; Willner, I. *Chem. Eur. J.* **1998**, *4*, 1068. (e) Katz, E.; Heleg-Shabtai, V.; Bardea, A.; Willner, I.; Rau, H. K.; Haehnel, W. *Biosens. Bioelectron.* **1998**, *13*, 741.

(9) Riklin, A.; Katz, E.; Willner, I.; Stocker, A.; Bückmann, A. F. *Nature* **1995**, *376*, 672.

(10) Zahavy, E.; Willner, I. *J. Am. Chem. Soc.* **1996**, *118*, 12499.

(11) (a) DeGrado, W. F.; Wassermann, Z. R.; Lear, J. D. *Science* **1989**, *243*, 622. (b) Mutter, M.; Vuilleumier, S. *Angew. Chem., Int. Ed. Engl.* **1989**, *28*, 535. (c) Bryson, J. W.; Betz, S. F.; Lu, H. S.; Suich, D. J.; Zhou, H. X.; O′Neil, K. T.; DeGrado, W. F. *Science* **1995**, *270*, 935. (d) Hill, R. B.; DeGrado, W. F. *J. Am. Chem. Soc.* **1998**, *120*, 1138. (e) Gilney, B. R.; Mulholland, S. E.; Rabanal, F.; Dutton, P. L. *Proc. Natl. Acad. Sci. U.S.A.* **1996**, *93*, 15041.

(12) (a) Choma, C. T.; Lear, J. D.; Nelson, M. J.; Dutton, P. L.; Robertson, D. E.; DeGrado, W. F. *J. Am. Chem. Soc.* **1994**, *116*, 856. (b) Robertson, D. E.; Farid, R. S.; Moser, C. C.; Urbauer, J. L.; Mulholland, S. E.; Pidikiti, R.; Lear, J. D.; Wand, A. J.; DeGrado, W. F.; Dutton, P. L. *Nature* **1994**, *368*, 425. (c) Rabanal, F.; DeGrado, W. F.; Dutton, P. L. *J. Am. Chem. Soc.* **1996**, *118*, 473. (d) Arai, F.; Kobata, K.; Mihara, H.; Fujimoto, T.; Nishino, N. *Bull. Chem. Soc. Jpn.* **1995**, *68*, 1989.

(13) Mutter, M.; Altmann, E.; Altmann, K.-H.; Hersperger, R.; Koziej, P.; Nebel, K.; Tushscherer, G.; Vuilleumier, S.; Gremlich, H. U.; Müller, K. *Helv. Chim. Acta* **1988**, *71*, 835.

(14) Rau, H. K.; Haehnel, W. *J. Am. Chem. Soc.* **1998**, *120*, 468.

(15) Katz, E.; Heleg-Shabtai, V.; Willner, I.; Rau, H. K.; Haehnel, W. *Angew. Chem., Int. Ed. Engl.* **1998**, *37*, 3253.

(16) Ascoli, F.; Rosaria, M.; Fanelli, R.; Antonini, E. In *Methods in Enzymology;* Antonini, E., Rossi-Bernardi, L., Chiancone, E., Eds.; Academic Press: London, 1981; Vol. 76, p 72.

(17) Ikeda, N. *Pharm. J. Soc. Jpn.* **1955**, *75*, 645.

(18) Katz, E.; Solov'ev, A. A. *J. Electroanal. Chem.* **1990**, *291*, 171.

(19) Katz, E.; Schlereth, D. D.; Schmidt, H.-L. *J. Electroanal. Chem.* **1994**, *367*, 59.

(20) Woods, R. In *Electroanalytical Chemistry*; Bard, A. J., Ed.; Marcel Dekker: New York, 1980; vol. 9, p 1.

Scheme 1. Stepwise Assembly of the Fe(III)−Protoporphyrin IX-Reconstituted de Novo Protein on the Maleimide Monolayer-Functionalized Au electrode

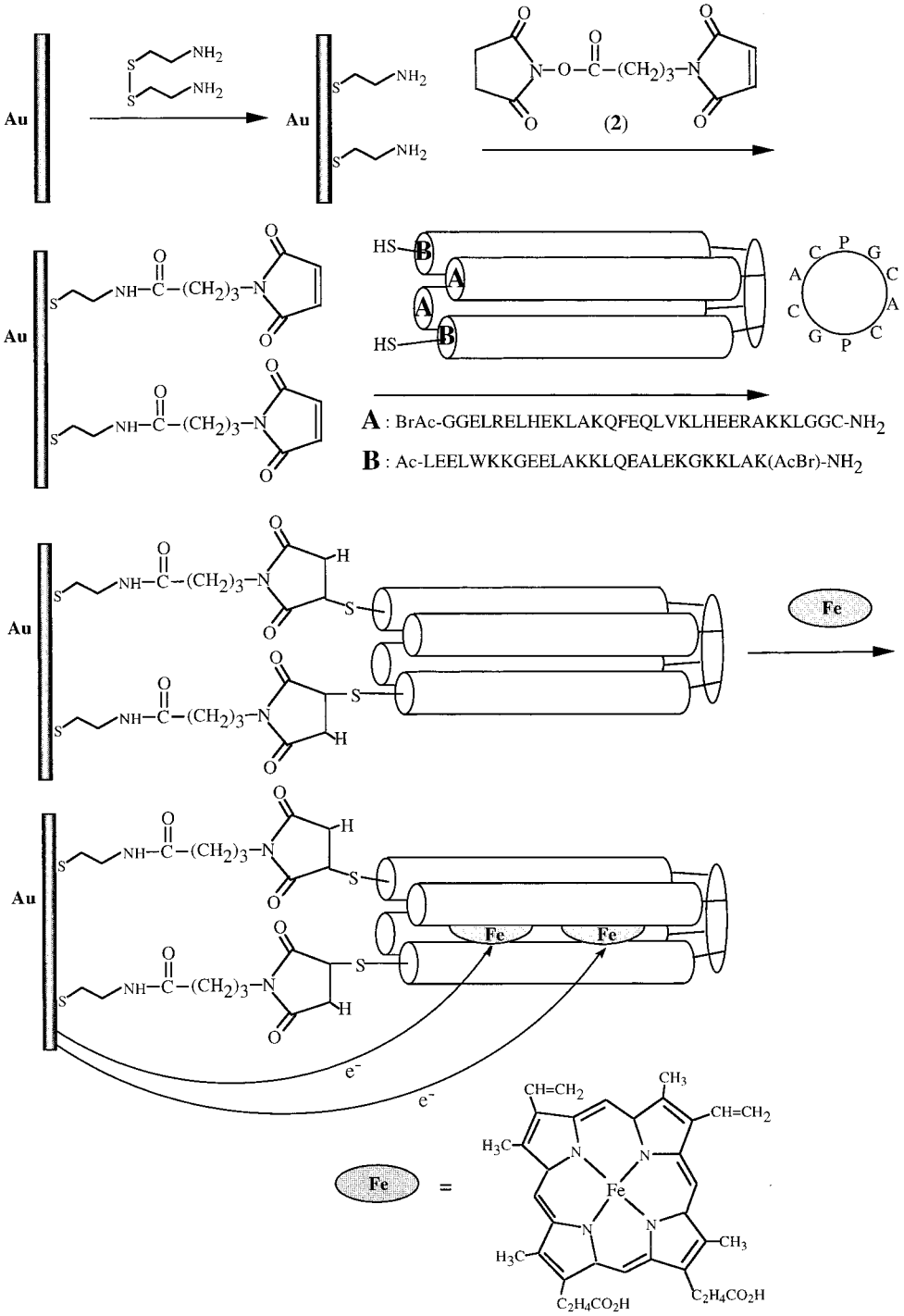

by its rinsing with DMSO. In the appropriate experiments, reconstitution of the de novo protein with two Fe(III) heme sites was performed in a solution consisting of the de novo protein and Fe(III)−protoporphyrin IX followed by purification as described previously.[14] The de novo protein that includes the two Fe(III) heme sites was then used for its immobilization on the maleimide-functionalized Au electrode as described above.

The Au electrode functionalized with the de novo protein monolayer reconstituted with the Fe(III) heme was used for further deposition of the biocatalytic proteins: nitrate reductase or Co(II)−Mb. In these experiments, the Au support was roughened as described above prior to the modification step with cystamine. The Fe(III) heme-reconstituted de novo protein-modified Au-roughened electrode was soaked in the respective protein solution (0.1 unit/mL of nitrate reductase or 3.5×10^{-4} M Co(II)−Mb) in 0.1 M phosphate buffer, pH 7.0, for 20 min, and briefly rinsed (2 s) in the phosphate buffer. Then the electrode was treated with a 10% (v/v) aqueous glutaric dialdehyde solution and rinsed well with the phosphate buffer.

Reversible binding of the de novo protein to a Au electrode included the reaction of a cystamine-modified Au electrode (roughness factor ca. 1.5) with 1×10^{-3} M *p*-hydroxymercury benzoic acid in 0.1 M HEPES buffer, pH 7.3, in the presence of 2×10^{-3} M EDC, for 2 h. Then the electrode was reacted with the de novo protein that included two Fe(III) heme sites, 0.5 mg mL^{-1}, in 0.1 M phosphate buffer, pH 7.0, for 2 h. To split the Hg−S bonds connecting the de novo protein from the surface, the electrode was reacted with 1×10^{-3} M mercaptoethanol in 0.1 M phosphate buffer, pH 7.0, for 30 min. The redeposition of the de novo protein on the electrode surface that was

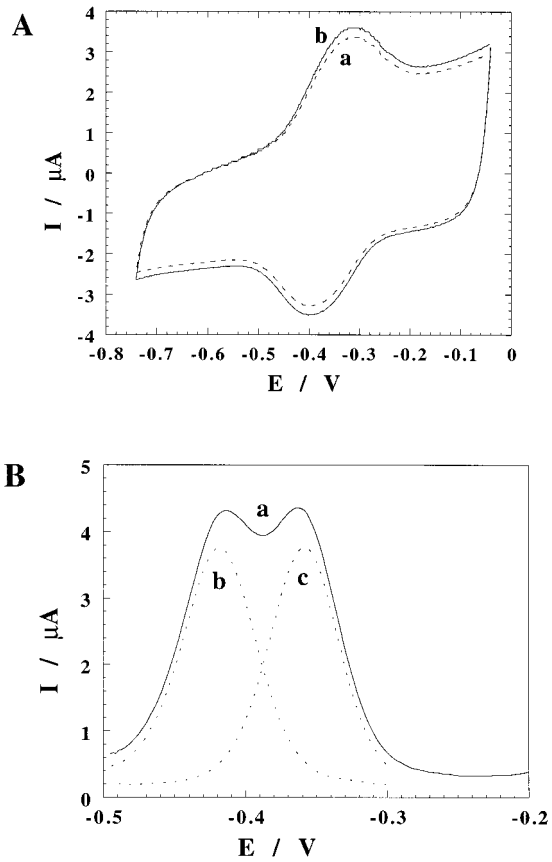

Figure 1. (A) Cyclic voltammograms of the Fe(III)−protoporphyrin-reconstituted de novo protein-functionalized Au electrode: reconstitution with Fe(III)−protoporphyrin IX was performed before (a) or after (b) de novo protein immobilization on the maleimide-functionalized Au electrode. Potential scan rate 200 mV·s^{-1}. (B) Differential pulse voltammogram (a) and deconvoluted voltammograms (b, c) of the Fe(III)-reconstituted de novo protein-functionalized Au electrode. Potential scan rate 20 mV·s^{-1}, pulse height 2 mV. The cyclic voltammograms and differential pulse voltammograms were recorded under argon in the background electrolyte: 0.1 M phosphate buffer, pH 7.0; Au electrode with a geometrical area of ca. 0.2 cm^2 and a roughness factor of ca. 1.3.

already treated with mercaptoethanol was performed in the presence of 0.5 mg mL^{-1} de novo protein solution (0.1 M phosphate buffer, pH 7.0) for 24 h.

To estimate the Au surface coverage with the maleimide groups, the maleimide-functionalized electrode was reacted with cysteamine (2-aminoethyl thiol), 1×10^{-4} M for 5 min, rinsed with water, and then reacted with 2-chloro-3-(3-carboxypropylamine)-1,4-naphthoquinone (**1**), 1×10^{-3} M, in the presence of 2×10^{-3} M EDC in HEPES buffer, pH 7.3, for 2 h.

Measurements. Electrochemical measurements (cyclic voltammetry, differential pulse voltammetry, chronoamperometry, and amperometry under constant applied potential) were performed using a potentiostat (EG&G VersaStat) connected to a personal computer (EG&G research electrochemistry software model 270/250). All the measurements were carried out at ambient temperature (22 ± 2 °C) in a conventional three-compartment electrochemical cell consisting of the chemically modified Au electrode as a working electrode, a glassy carbon auxiliary electrode isolated by a glass frit, and a saturated calomel electrode (SCE) connected to the working volume with a Luggin capillary. All potentials are reported with respect to this reference electrode. Argon bubbling was used to remove oxygen from the solution in the electrochemical cell. Phosphate buffer (0.1 M, pH 7.0) was used as a background electrolyte.

A rotating disk electrode (RDE) (4.5 mm diameter) was polished with an alumina suspension (0.3 μm, Buehler, IL), rinsed with water,

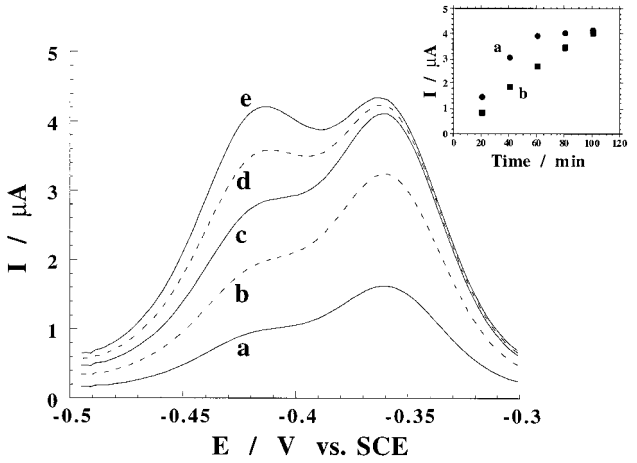

Figure 2. Differential pulse voltammograms recorded after different times of interaction of the de novo protein monolayer−Au electrode with the Fe(III)−protoporphyrin IX solution (1×10^{-4} M in DMSO): (a) 20 min, (b) 40 min, (c) 60 min, (d) 80 min, and (e) 100 min. The experiment was performed under argon in the background electrolyte: 0.1 M phosphate buffer, pH 7.0; potential scan rate 20 mV·s^{-1}; pulse height 2 mV; Au electrode with a geometrical area of ca. 0.2 cm^2 and a roughness factor of ca. 1.3. Inset: Peak currents of the more negative heme (b) and less negative heme (a) as a function of the reconstitution time.

and then modified in the same way as the Au wire electrodes. The RDE measurements were performed with an electrode rotator (model 636 EG&G). The rate of rotation was increased stepwise, and after each step the cathodic current was measured when it had stabilized (after a few seconds).

Constant-potential electrolysis was applied using the Fe(III) heme-reconstituted de novo protein monolayer−Au electrode integrated with nitrate reductase, or with Co(II)−Mb in the presence of nitrate, 0.1 M, or acetylenedicarboxylic acid, 0.1 M, respectively. Nitrite formed upon bioelectrocatalytic reduction of nitrate was quantitatively analyzed by a spectrometric method based on diazotization of sulfanilamide and coupling with *N*-1-naphthylethylenediamine dihydrochloride. Samples (100 μL) of the cell solution were transferred at time intervals of electrolysis into a cuvette; then 1 mL of each of the reagents was added, and the absorption at $\lambda = 540$ nm was measured after 10 min of reaction. The concentration of maleic acid produced upon bioelectrocatalytic hydrogenation of acetylenedicarboxylic acid was determined by HPLC, using a Merck-Hitachi instrument equipped with a Shodex KC-811 ionpack column (0.1% H_3PO_4) and an optical detector (190−370 nm).

A quartz crystal microbalance analyzer (QCM) (EG&G model QCA 917) linked to a personal computer was employed for the microgravimetric analyses. Quartz crystals (AT-cut, EG&G, fundamental frequency ca. 9 MHz) sandwiched between two Au electrodes (area ca. 0.196 cm^2; roughness factor ca. 3.5) were used. Modification of the Au/quartz crystal was carried out by procedures identical to those employed for the Au wire electrodes.

Results and Discussion

The structure of the synthetic de novo protein was published recently,[14] and it is schematically shown in Scheme 1. The protein consists of 128 amino acids, and it has a mass of 14 728 Da. Flexible Gly-Gly-Cys units are part of the helices B, and they provide a means for the covalent attachment of the protein to an electrode surface (vide infra). The de novo protein includes four histidine units, two in each of the helices A. The histidine units are positioned on opposite helices to allow axial ligation of Fe(III) heme sites to the protein assembly. The method for assembling the de novo protein on a Au electrode is shown in

(21) (a) Laviron, E. *J. Electroanal. Chem.* **1979**, *101*, 19. (b) Laviron, E.; Roullier, L. *J. Electroanal. Chem.* **1980**, *115*, 65.

Scheme 1. A cystamine monolayer associated with a Au electrode was reacted with the bifunctional reagent *N*-succinimidyl-3-maleimidopropionate (**2**) to yield a maleimide-functionalized monolayer electrode. The resulting electrode was then reacted with the cysteine-modified de novo protein to yield the four-helix bundle protein monolayer on the electrode surface. The intermediate maleimide-functionalized electrode was characterized by its stepwise reaction with cysteine and then by the covalent coupling of the naphthoquinone carboxylic derivative (**1**).[18] By coulometric assay of the reduction (or oxidation) of the quinone, and assuming that two electrons are involved in the reduction process, we estimate its surface coverage to be 4.8×10^{-11} mol·cm^{-2}. This value should be considered as a lower limit for the surface coverage of the electrode by the maleimide residues. Nonetheless, further attempts to react the maleimide monolayer with thiol-functionalized redox-active substrates failed to yield further noticeable modification of the monolayer, suggesting that all of the maleimide residues reacted with the quinone sites. The resulting de novo protein monolayer was interacted with Fe(III)−protoporphyrin IX. Figure 1A (curve a) shows the cyclic voltammogram of the resulting Fe(III)−protoporphyrin IX-reconstituted de novo protein monolayer. A single redox wave at a formal potential of ca. $E° = -0.35$ V, exhibiting a peak-to-peak separation of ca. $\Delta E = 80$ mV (200 mV·s^{-1}), is observed, and at higher scan rates, the peak-to-peak separation increases, as predicted theoretically.[21] Theoretical predictions[21] suggest that the peak-to-peak separation of a redox species confined to an electrode in a monolayer configuration, and lacking intermolecular interactions, is $\Delta E \approx 0$. Nonetheless, intermolecular interaction of the redox label in the monolayer array could increase the cathodic and anodic peak separation.[21b] It should be noted that the de novo protein monolayer without reconstitution with Fe(III)−protoporphyrin IX does not show any electrochemical activity. Differential pulse voltammetry reveals that the electrical response of the heme(s) reconstituted into the de novo protein consists of two waves, Figure 1B, curve a. The two overlapping redox waves are deconvoluted to two separate electrochemical processes of two distinct and different heme sites: The reduction potential of one of the heme centers is $E° = -0.43$ V, whereas the reduction potential of the second heme site is positively shifted by ca. 70 mV and appears at ca. $E° = -0.36$ V. These values are in complete agreement with redox potentials of the two Fe(III)−protoporphyrin IX sites reconstituted into the de novo protein and assayed by potentiometric titration[14] ($E_1° = -0.352$ V and $E_2° = -0.412$ V vs SCE). Comparison of the deconvoluted redox peaks of the two heme sites reveals that the two Fe(III)−protoporphyrin IX units are associated with the four-helix bundle at a 1:1 ratio, Scheme 1. The de novo protein was reconstituted in solution with Fe(III)−protoporphyrin IX, and the resulting synthetic protein was covalently coupled to the maleimide monolayer. Figure 1A, curve b, shows the cyclic voltammogram of the resulting monolayer electrode. The cyclic voltammogram overlaps that obtained upon interaction of the de novo protein monolayer electrode with the metal porphyrin, implying that surface reconstitution of the synthetic de novo protein monolayer on the electrode surface yields a hemoprotein that is identical to that obtained upon reconstitution of the synthetic protein in solution. Coulometric assay of the redox wave that corresponds to the de novo protein with the two heme sites indicates that its surface coverage is ca. 2.5×10^{-11} mol·cm^{-2}. Assuming[14] that the protein diameter consisting of the four-helix bundle assembly is ca. 25 Å^2, the footprint of the protein cylinder is ca. 6.25×10^{-14} cm^2. Thus, the theoretical surface coverage of a dense monolayer of the de novo protein is ca. 3.5×10^{-11} mol·cm^{-2}. Thus, the experimental surface coverage of the de novo synthesized protein is about 70% of the theoretical coverage of the densely packed monolayer, and it is half of the surface density of the maleimide anchoring sites. On the basis of these results, we suggest that the four-helix bundle protein is attached to the maleimide residues via its two cysteine bridging units as a tentative configuration. Figure 2 shows the differential pulse voltammetry waves of the de novo protein monolayer−electrode upon interaction with Fe(III)−protoporphyrin IX for different time intervals. It is evident that the heme site exhibiting the slightly more negative redox potential reconstitutes more slowly

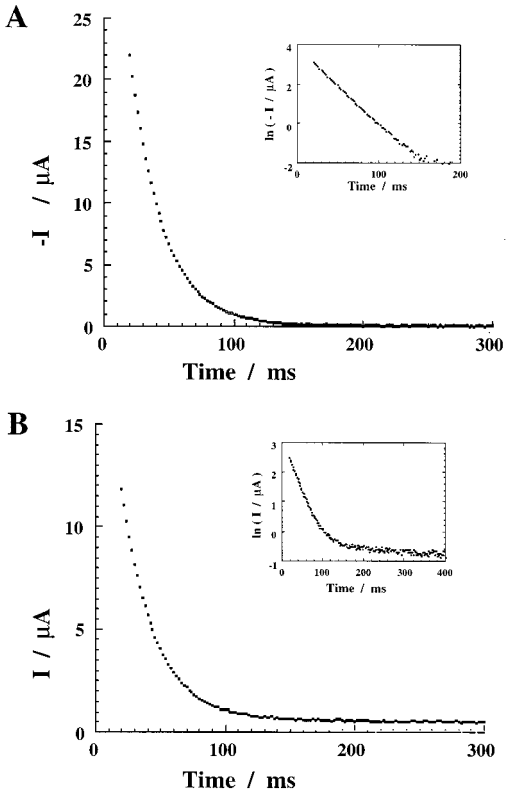

Figure 3. (A) Current decay upon application of the negative potential step (from −0.2 to −0.45 V) resulting in the reduction of both heme sites in the Fe(III)−protoporphyrin IX-reconstituted de novo protein monolayer. The inset shows the semilogarithmic plot of the current decay. (B) Current decay upon application of the positive potential step (from −0.57 to −0.32 V) resulting in the oxidation of both heme sites in the Fe(II)−protoporphyrin IX-reconstituted de novo protein monolayer. The inset shows the semilogarithmic plot of the current decay. The experiment was performed in 0.1 M phosphate buffer, pH 7.0, under argon; Au electrode with a geometrical area of ca. 0.2 cm^2 and a roughness factor of ca. 1.3.

Scheme 2. Vectorial Electron Transfer in the Two-Heme-Site-Reconstituted de Novo Protein Molecules

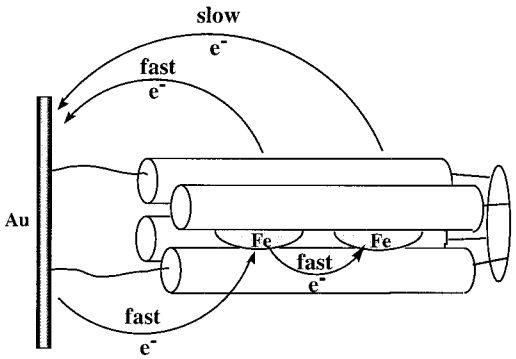

Scheme 3. Reversible Binding of the Fe(III)−Protoporphyrin IX-Reconstituted de Novo Protein to the Mercury Benzoate-Functionalized Au Electrode

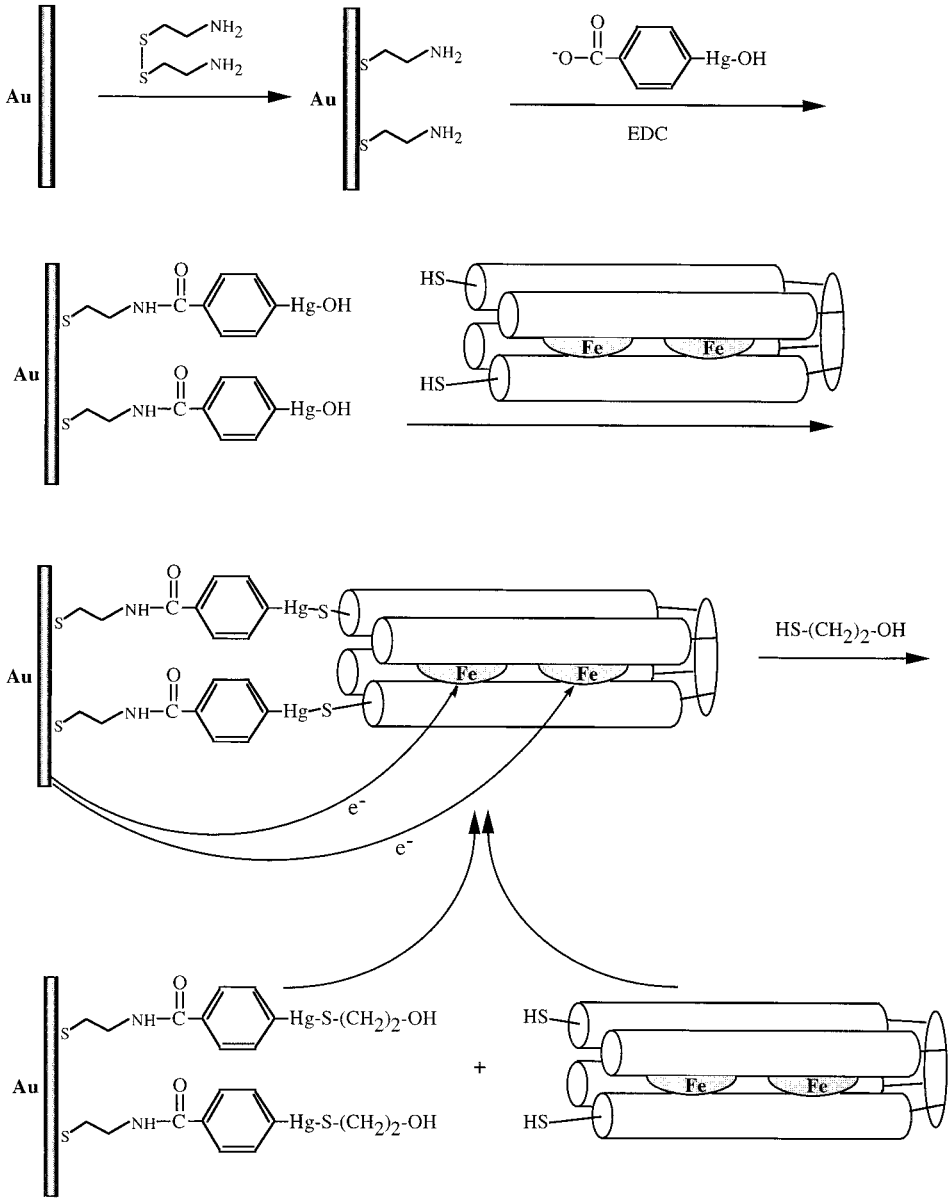

into the synthetic protein. Figure 2 (inset) shows the kinetics of the reconstitution of the Fe(III) heme sites exhibiting the more negative redox potential and more positive redox potential (curves b and a, respectively). It should be noted that the redox potentials of heme sites are controlled by the specific microenvironment of the protein.[22] Thus, the different redox potentials of the heme centers, which are reconstituted into the de novo protein assembly, can be attributed to different protein−heme interactions. In fact, recent EPR and ENDOR spectroscopy measurements[23] on the bis-heme de novo protein indicate that while one heme site is characterized by axial histidine ligands exhibiting parallel histidine planes, the other heme component includes histidine ligands with tilted or twisted histidine planes. Thus, the different redox potentials of the heme centers in the de novo protein could originate from the different histidine coordination geometries.

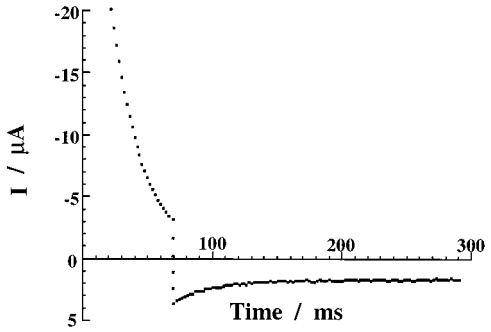

Figure 4. Transient current recorded with the Fe(III)−protoporphyrin IX-reconstituted de novo protein monolayer during the double-potential step chronoamperometric experiment. The potential steps from −0.2 to −0.5 V to reduce the hemes in the protein, and after 70 ms the potential steps back, from −0.5 to −0.2 V to oxidize the reduced hemes. The experiment was performed in 0.1 M phosphate buffer, pH 7.0, under argon; Au electrode with a geometrical area of ca. 0.2 cm^2 and a roughness factor of ca. 1.3.

(22) Tezcan, F. A.; Winkler, J. R.; Gray, H. B. *J. Am. Chem. Soc.* **1998**, *120*, 1338.

(23) Fahnenschmidt, M.; Rau, H. K.; Bittl, R.; Haehnel, W.; Lubitz, W. *Chem. Eur. J.*, in press.

Scheme 4. Electrocatalaytic Reduction of Cytochrome *c* via Vectorial Electron Transfer in the Heme-Reconstituted de Novo Protein Monolayer

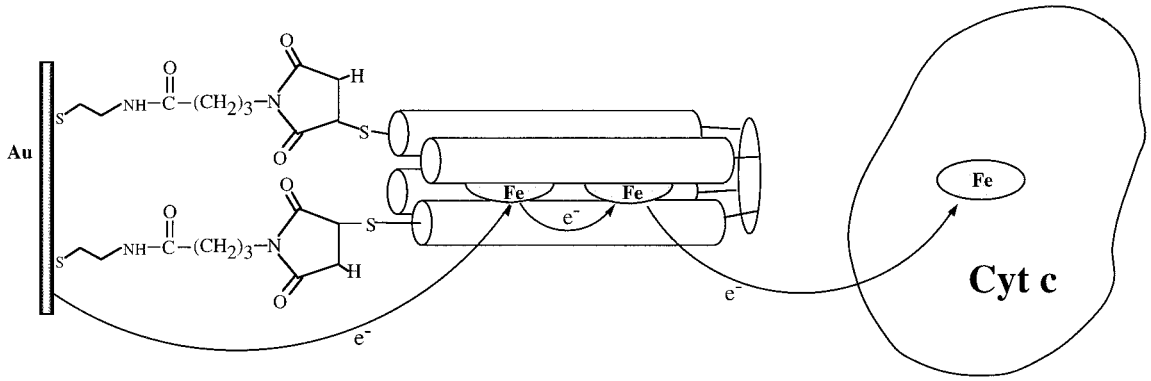

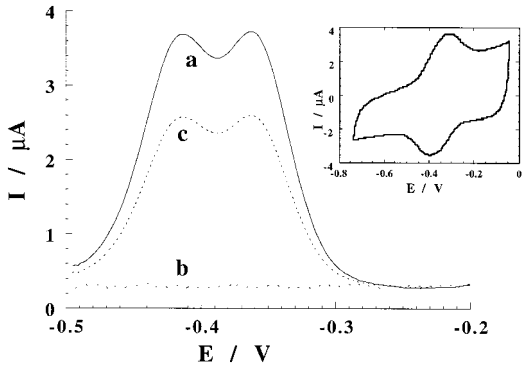

Figure 5. Differential pulse voltammograms of the Fe(III)−protoporphyrin IX-reconstituted de novo protein-modified Au electrode: (a) after binding the Fe(III)−protoporphyrin IX-reconstituted de novo protein to mercury benzoate groups on the electrode surface, (b) after treating the electrode with mercaptoethanol, (c) after secondary attachment of the de novo protein. Inset: cyclic voltammogram of the Au electrode modified with the Fe(III)−protoporphyrin IX-reconstituted de novo protein bound to the electrode via mercury benzoate groups. Potential scan rate 200 mV·s^{-1}; Au electrode with a geometrical area of ca. 0.2 cm^2 and a roughness factor of ca. 1.3.

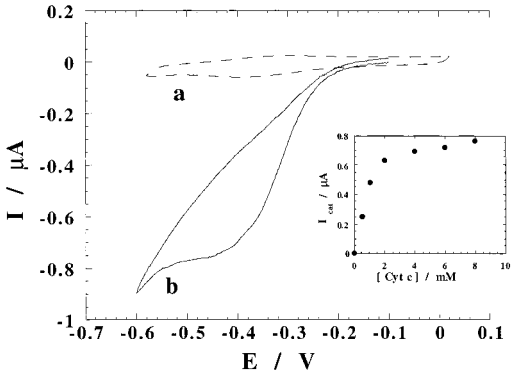

Figure 6. Cyclic voltammograms of the Fe(III)−protoporphyrin IX-reconstituted de novo protein-modified Au electrode in the absence (a) and presence (b) of cytochrome *c* (5 mM). The experiment was performed under argon in 0.1 M phosphate buffer, pH 7.0. Potential scan rate 5 mV·s^{-1}; Au electrode with a geometrical area of ca. 0.2 cm^2 and a roughness factor of ca. 1.3. Inset: the electrocatalytic current (at $E = -0.5$ V) as a function of the cytochrome *c* concentration.

To identify the position of the Fe(III)−protoporphyrin IX units in the de novo synthesized protein assembly, we applied chronoamperometric experiments.[24] Previous studies[25] have indicated that the interfacial electron-transfer rates to or from redox sites associated with the electrode support are controlled by the distance separating the redox species and the electrode. As the distance separating the redox component and the electrode increases, the interfacial electron-transfer rate decreases. Thus, for the two heme sites, reconstituted into the synthetic protein and positioned at different distances, we expect a biexponential current decay upon the reduction of the assembly, Scheme 1. A fast electron transfer should occur to the heme site positioned near the electrode surface, while a slow electron transfer is expected to the second heme center in the remote position, with respect to the electrode. Figure 3A shows the transient current response upon the reduction of the Fe(III)−protoporphyrin IX-reconstituted protein assembly. Kinetic analysis of this curve, Figure 3A (inset), reveals a single exponent electron-transfer rate constant, $k_{et} = 40$ s^{-1} (at −0.45 V vs SCE). This result is attributed to the vectorial electron transfer occurring in the bifunctional Fe(III)−protoporphyrin IX-reconstituted protein array, Scheme 2. The Fe(III) heme site close to the electrode support exhibits the more negative redox potential (−0.43 V). Rapid electron transfer to the heme site near the electrode is accompanied by a fast intramolecular electron transfer to the second heme center (−0.36 V), due to the potential gradient existing between the two heme sites. Thus, the electron-transfer rate of the entire assembly is controlled by the primary electron-transfer rate to the heme site close to the electrode. It should be noted that the heterogeneous electron-transfer rate constant to the heme site close to the electrode surface is controlled by the potential applied on the electrode support. Thus, the rate of the electron-transfer cascade leading to the reduction of the de novo protein assembly can be regulated by the potential applied on the electrode. Two important conclusions can be drawn from the analysis of the redox behavior and the kinetic analysis of the electron transfer of the reconstituted protein at the electrode surface: (i) The microenvironment of the amino acids surrounding the heme sites influences the redox potential of the heme center. (ii) The kinetic analysis of the interfacial electron transfer and the identification of the vectorial electron-transfer cascade enable the identification of the positions of the two Fe(III)−protoporphyrin sites in the de novo protein assembly. The heme site exhibiting the more negative reduction potential is positioned near the electrode support, whereas the second heme center is in a remote position with respect to the electrode and close to the cyclic peptide frame that ties together the four-helix bundle.

The fact that the heme site near the electrode exhibits the more negative reduction potential implies, however, that the pulsed oxidation of the reduced bifunctional heme assembly

(24) Katz, E.; Willner, I. *Langmuir* **1997**, *13*, 3364.

(25) (a) Chidsey, C. E. D. *Science* **1991**, *251*, 919. (b) Katz, E.; Itzhak, N.; Willner, I. *Langmuir* **1993**, *9*, 1392. (c) Guo, L.-H.; Facci, J. S.; McLendon, G. *J. Phys. Chem.* **1995**, *99*, 8458.

Scheme 5. Assembly of the Integrated Nitrate Reductase/Fe(III)−Protoporphyrin IX-Reconstituted de Novo Protein-Layered Au Electrode

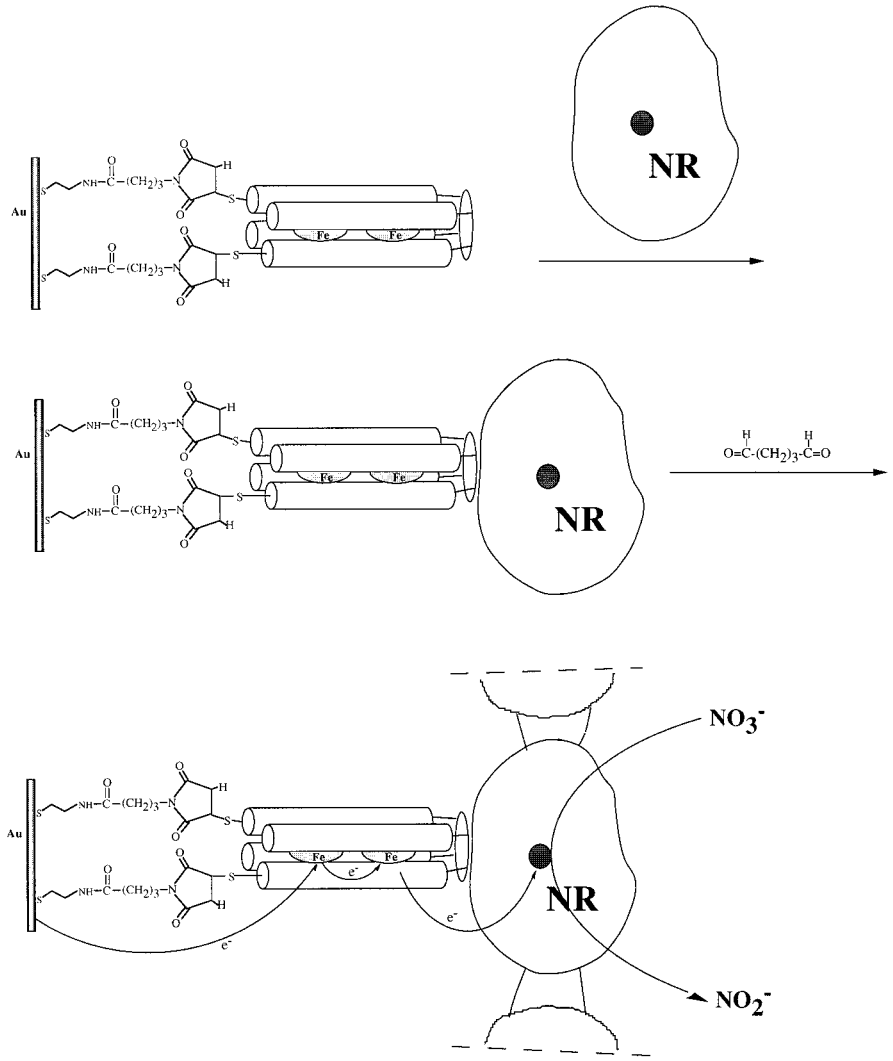

would proceed via two independent routes of different kinetics, Scheme 2. That is, oxidation of the reduced bifunctional Fe(II)−protoporphyrin IX-reconstituted de novo protein cannot proceed by an intramolecular path, and the two reduced sites are oxidized independently with different electron-transfer kinetics. The transient current response[26] will have a biexponential time dependence as expressed by eq 1, where Q_1 and

$$I(t) = (Q_1 k_{et}^{\ 1})e^{-k_{et}^{1}t} + (Q_2 k_{et}^{\ 2})e^{-k_{et}^{2}t} \qquad (1)$$

Q_2 correspond to the charge associated with the oxidation of the two heme centers and k_{et}^1 and k_{et}^2 are the interfacial electron-transfer rates between the heme site close to the electrode surface and the heme center positioned at the remote site relative to the electrode support, respectively. Figure 3B shows the transient anodic current response upon the pulsed oxidation of the Fe(II)−protoporphyrin IX-reconstituted de novo protein assembly. Figure 3B (inset) shows the kinetic analysis of the resulting transient current response. The transient current follows biexponential kinetics, $k_{et}^1 = 40\ s^{-1}$, $k_{et}^2 = 1.0\ s^{-1}$, and the respective preexponential factors indicate that the Q_1:Q_2 ratio is 1:1.[27] The surface density of the more negative or more positive heme site derived from Q_1 or Q_2, respectively, is ca. 2.5×10^{-11} mol·cm^{-2}, identical to the surface coverage value of the hemoprotein on the electrode extracted by the coulometric assay of its cyclic voltammogram. The fast component of the transient anodic current is attributed to the oxidation of the reduced heme site close to the electrode surface, while the slow component of the anodic current belongs to the oxidation of the heme site in the remote position relative to the electrode surface. It should be noted that although we do not apply in the chronoamperometric experiments an overpotential for the complete reduction (or the oxidation) of the two heme centers, the coulometric assay (or the determination of the surface coverage) of the two heme sites is possible by the kinetic analysis of the transient currents,[24,26] and the determination of the respective preexponential factors, eq 1.

The reduction of the Fe(III)−protoporphyrin de novo protein assembly proceeds by a fast unidirectional route that reduces the remote heme center. The oxidation of the reduced assembly

(26) (a) Forster, R. J. *Langmuir* **1995**, *11*, 2247. (b) Forster, R. J.; Faulkner, L. R. *Anal. Chem.* **1995**, *67*, 1232. (c) Forster, R. J. *Anal. Chem.* **1996**, *68*, 3143. (d) Forster, R. J. *Analyst* **1996**, *121*, 733.

(27) The applied potential step provides an overpotential that corresponds to 130 and 40 mV with respect to the heme sites close to and remote from the electrode support, respectively. According to the Nernst equation, these overpotential values lead to the complete oxidation of the heme center close to the electrode, and to 80% of the oxidation of the remote heme site. These values were taken into account in calculating the Q_1 and Q_2 values.

to the Fe(III)−protoporphyrin IX occurs by the separate oxidation of the two heme sites, and particularly through the slow oxidation of the heme center located in the remote position of the de novo protein, relative to the electrode support. These results suggest that the Fe(III)−protoporphyrin IX-reconstituted de novo protein monolayer assembled on the electrode surface can act as a rectifier system, Figure 4. A double-step chronoamperometric experiment was performed to demonstrate the rectifier function of the system. The potential applied to the Fe(III)−porphyrin−protein assembly was stepped from −0.2 to −0.5 V, and the step was interrupted after 70 ms. The reverse step from −0.5 to −0.2 V was then applied to oxidize the reduced assembly. The duration of the cathodic step was tuned to allow a single electron transfer per protein assembly. As previously indicated, the heme center near the electrode surface is rapidly reduced, and it mediates very fast electron transfer to the second heme site due to the potential gradient existing in the system. Thus, upon the application of the cathodic step and the transfer of a single electron to the assembly, a fast cathodic current decay is observed, and the electron is ultimately positioned on the remote heme site. Upon the application of the reverse step, the system exists in a configuration where the heme center close to the electrode is in the Fe(III) state, whereas the remote metal−porphyrin site is in the reduced Fe(II) state. Upon the application of the oxidation step, only the very slow oxidation of the remote Fe(II)−porphyrin center is observed, giving rise to the very slow recovery of the initial assembly. Thus, the system operates as a rectifier and reveals fast unidirectional electron transfer and slow electron transfer in the reverse direction.

A further aspect that was addressed in our study involves the development of other routes to immobilize the de novo synthesized hemoprotein on the electrode support, and particularly to develop means to regenerate the protein monolayer−electrode. It should be noted that we have emphasized the immobilization of the thiolated de novo protein by its covalent attachment to maleimide residues comprising the base monolayer. Attempts to directly immobilize the de novo protein onto the Au surface failed to yield a protein monolayer that could be reconstituted with Fe(III)−protoporphyrin IX. Thus, our results imply that the primary assembly of a monolayer on the electrode support is important for minimizing the direct interactions between the protein and the electrode surface. Scheme 3 shows an alternative method to generate the Fe(III)−protoporphyrin IX-reconstituted protein monolayer on the electrode surface. The cystamine monolayer associated with a Au electrode was coupled to *p*-hydroxymercury benzoic acid that provides active sites for highly specific and reversible binding of the thiol groups.[28] The resulting functionalized monolayer was reacted with the cysteine-modified Fe(III)−protoporphyrin IX-reconstituted de novo protein. Figure 5, curve a, shows the differential pulse voltammogram of the hemoprotein monolayer. Figure 5 (inset) shows the cyclic voltammogram of the resulting monolayer. Coulometric assay of the reduction (or oxidation) waves of the reconstituted protein reveals a surface coverage almost identical to that obtained upon the modification of the maleimide monolayer with the synthetic protein, ca. 2.3×10^{-11} mol·cm^{-2}. Reaction of the resulting hemoprotein-functionalized monolayer with mercaptoethanol results in the differential pulse voltammogram shown in Figure 5, curve b. The redox responses of the heme sites are depleted, indicating that the Fe(III)−porphyrin-functionalized protein is displaced from the monolayer. Further interaction of the monolayer-functionalized electrode with the cysteine-modified Fe(III)−protoporpyhyrin IX-reconstituted protein results in the differential pulse voltammogram shown in Figure 5, curve c. The redox response of the hemoprotein is partially restored, indicating that it re-forms the mercury-thiolated protein bonds. The voltammogram obtained upon the secondary immobilization of the hemoprotein reveals, however, that only ca. 65% of the initial protein layer on the electrode is recovered after 24 h. The secondary immobilization of the de novo protein on the modified electrode surface proceeds very slowly since it requires substitution of the mercaptoethanol bound to the mercury benzoate monolayer. These results demonstrate that the *p*-hydroxymercury benzoate monolayer provides an active interface for the covalent attachment of thiolated proteins, and enables the cyclic regeneration of the protein layer.

Cytochrome *c* is a low molecular weight hemoprotein that acts as electron-transfer mediator for various redox enzymes.[29] Recently, we demonstrated that a microperoxidase-11 monolayer-modified Au electrode can provide electrocatalytic reduction of cytochrome *c*.[30] The redox potential of Cyt *c*[31] is $E^\circ = 0.01$ V, and thus the Fe(III)−protoporphyrin IX-reconstituted de novo protein could mediate electron transfer to Cyt *c*. The synthetic bifunctional hemoprotein assembled onto the Au electrode via the maleimide bridge, Scheme 4, was interacted with Cyt *c*. Figure 6, curves a and b, shows the cyclic voltammograms of the synthetic hemoprotein monolayer−electrode in the absence and presence of Cyt *c*, respectively. Note that the cyclic voltammogram of the synthetic de novo protein is hardly visible due to the slow scan rate. In the presence of Cyt *c*, an electrocatalytic cathodic current is observed at the redox potential of the synthetic hemoprotein. Figure 6 (inset) shows the resulting electrocatalytic cathodic current at different concentrations of Cyt *c*. The cathodic current increases as the concentration of Cyt *c* is elevated, and it levels off to a constant saturation value at a concentration of Cyt *c* corresponding to ca. 4×10^{-3} M. These results suggest that electron transfer from the synthetic hemoprotein monolayer to Cyt *c* occurs by the formation of an affinity complex between the compounds. Upon saturation of the de novo hemoprotein monolayer with Cyt *c*, the saturation value of the cathodic current is observed.

Nitrate reductase, NR (cytochrome dependent, E.C. 1.9.6.1 from *Escherichia coli*), is a non-heme metalloprotein that participates in nitrate respiration.[32] The enzyme is of spherical shape and consists of two subunits (MW ≈ 142 000 and 58 000). It includes a molybdenum atom and ca. 40 iron atoms per enzyme unit. The enzyme utilizes cytochrome b_1 as native electron donor. We recently reported on the electrocatalytic reduction of NR using a microperoxidase-11 monolayer-modified electrode.[30] We have attempted to use the de novo hemoprotein assembled on the electrode and outlined in Scheme 1 as a functionalized interface to mediate electron transfer to NR and to activate the biocatalyst for the reduction of nitrate.

(28) Katz, E.; Solov'ev, A. A. *J. Electroanal. Chem.* **1989**, *261*, 217.

(29) (a) Hill, H. A. O.; Walton, N. J.; Higgins, I. J. *FEBS Lett.* **1981**, *126*, 282. (b) Lion-Dagan, M.; Katz, E.; Willner, I. *J. Chem. Soc., Chem. Commun.* **1994**, 2741. (c) Jin, W.; Wollenberger, U.; Bier, F. F.; Makower, A.; Scheller, F. W. *Bioelectrochem. Bioenerg.* **1996**, *39*, 221.

(30) Narvaez, A.; Dominguez, E.; Katakis, I.; Katz, E.; Ranjit, K. T.; Ben-Dov, I.; Willner, I. *J. Electroanal. Chem.* **1997**, *430*, 227.

(31) Taniguchi, I.; Toyosawa, K.; Yamaguchi, H.; Yasukouchi, K. *J. Chem. Soc., Chem. Commun.* **1982**, 1032.

(32) (a) Takahashi, H.; Taniguchi, S.; Egami, F. In *Comparative Biochemistry*; Florkin, M., Mason, H. S., Eds.; Academic Press: New York, 1963; Vol. 5, Chapter 2, p 91. (b) MacGregor, C. H. In *Methods in Enzymology*; Fleischer, S., Packer, L., Eds.; Academic Press: New York, 1978; Vol. 53, Chapter 37, p 347. (c) Payne, W. J. In *Methods in Enzymology*; Fleischer, S., Packer, L., Eds.; Academic Press: New York, 1978; Vol. 53, Chapter 60, p 634.

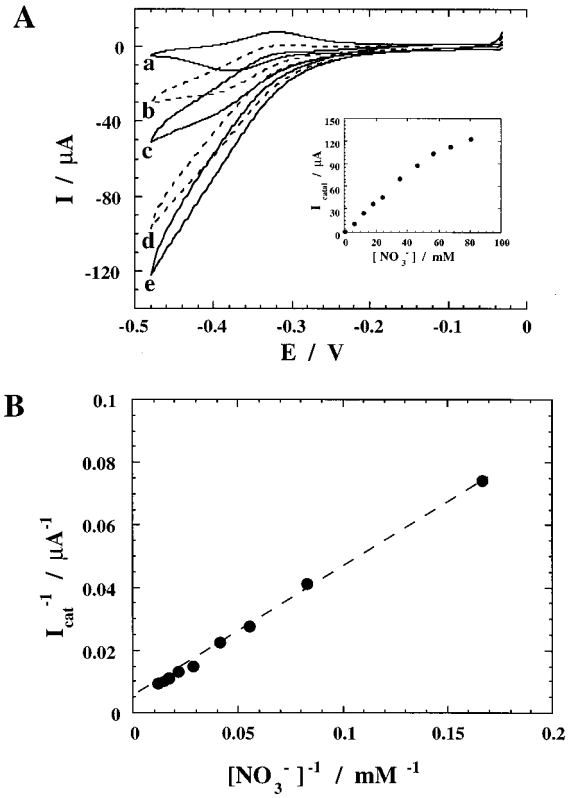

Figure 7. (A) Cyclic voltammograms of the integrated nitrate reductase/Fe(III)−protoporphyrin IX-reconstituted de novo protein-layered Au electrode at different concentrations of nitrate: (a) 0, (b) 12, (c) 24, (d) 46, and (e) 68 mM. Inset: calibration curve for the amperometric responses (at $E = -0.48$ V) of the electrode at different NO_3^- concentrations. Potential scan rate 5 mV·s^{-1}; 0.1 M phosphate buffer, pH 7.0; under argon; Au electrode roughness factor ca. 30; geometrical area ca. 2 cm^2. (B) Lineweaver−Burk analysis of the experimental calibration plot.

Addition of NR and nitrate (NO_3^-) to the de novo hemoprotein monolayer−electrode results in an electrocatalytic cathodic current and the electrocatalyzed formation of nitrite (NO_2^-). The catalytic current and the formation of NO_2^- are observed only upon the interaction of the functionalized monolayer−electrode with NR and NO_3^-. Elimination of any of these components prevents the formation of NO_2^-, indicating that mediated electron transfer from the de novo hemoprotein to NR activates the native biocatalyst for the reduction of NO_3^-. The limited amounts of NR and its high cost eliminate, however, the possibility of characterizing the system and, eventually, the use of the assembly as a nitrate biosensor. To overcome these difficulties, we attempted to tailor an integrated de novo hemoprotein monolayer/nitrate reductase−electrode as depicted in Scheme 5. The Fe(III)−protoporphyrin IX-reconstituted four-helix bundle protein assembled on the Au electrode was interacted with NR. As the native protein is negatively charged[32b] at pH 7.0, pI 4.2, and the de novo protein is positively charged at this pH, an electrostatic affinity complex between the two components is expected to form. Provided this affinity complex is sufficiently stable, then lateral, two-dimensional, cross-linking of the enzyme is anticipated to yield an integrated, electrically contacted, nitrate reductase film associated with the electrode. Figure 7A shows the cyclic voltammograms of the integrated de novo hemoprotein/NR-layered electrode in the absence of added nitrate (curve a), and in the presence of variable concentrations of nitrate, curves b−e. The electrocatalytic cathodic current observed at the potential of the de novo

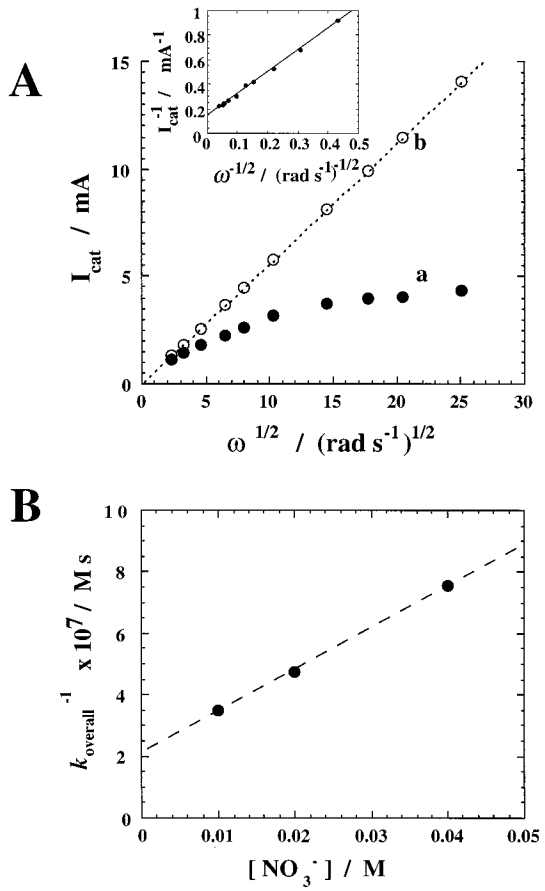

Figure 8. (A) Electrocatalytic currents corresponding to the reduction of 20 mM KNO_3 on the integrated nitrate reductase/Fe(III)−protoporphyrin IX-reconstituted de novo protein-layered Au rotating disk electrode vs $\omega^{1/2}$: (a) experimentally measured electrocatalytic currents at the applied potential $E = -0.5$ V, (b) theoretical Levich plot taking into account only diffusional limitations. Inset: Koutecky−Levich plot for the experimental electrocatalytic current. Background electrolyte 0.1 M phosphate buffer, pH 7.0; under argon; Au disk electrode roughness factor ca. 1.3. (B) Second-order rate constants ($k_{overall}$) for the reduction of NO_3^- extracted from the RDE measurements.

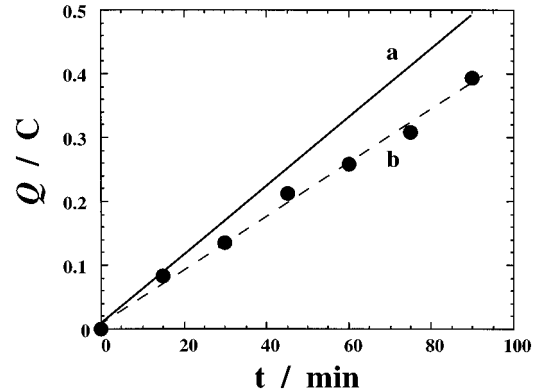

Figure 9. (a) Coulometric analysis of the charge passing the electrolyte cell during reduction of NO_3^- (0.1 M KNO_3) electrocatalyzed by the integrated nitrate reductase/Fe(III)−protoporphyrin IX-reconstituted de novo protein-layered Au electrode. (b) Calculated charge that passes the electrolyte cell according to the analyzed product, NO_2^-. Background electrolyte 0.1 M phosphate buffer, pH 7.0; under argon; applied potential $E = -0.5$ V; Au electrode with a geometrical area of ca. 2 cm^2 and a roughness factor of ca. 20.

hemoprotein implies that the synthetic protein mediates electron transfer to NR and activates the biocatalyst toward the electrocatalyzed reduction of nitrate (NO_3^-). Analysis of the reduction

Scheme 6. Assembly of the Co(II)−Myoglobin/Fe(III)−Protoporphyrin IX-Reconstituted de Novo Protein-Layered Au Electrode

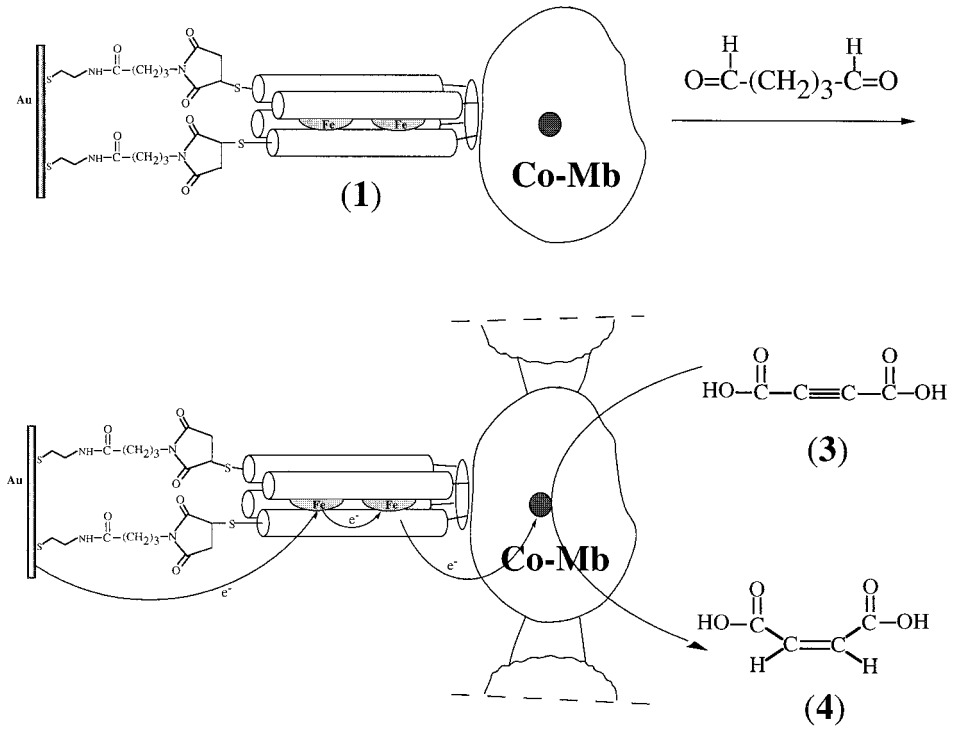

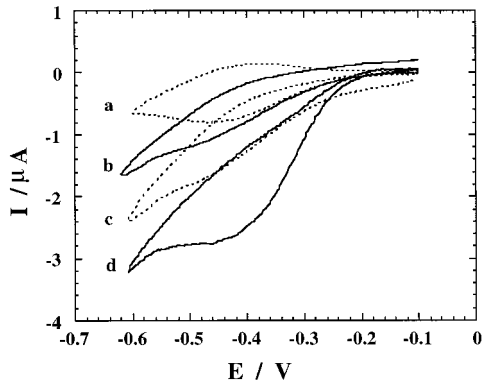

Figure 10. Cyclic voltammograms of the Fe(III)−protoporphyrin IX-reconstituted de novo protein-modified Au electrode in the presence of different concentrations of Co(II)−myoglobin: (a) 0 M; (b) 5×10^{-6} M; (c) 1×10^{-5} M; (d) 2×10^{-5} M. Background electrolyte 0.1 M phosphate buffer, pH 7.0; under argon; potential scan rate 5 mV·s^{-1}; Au electrode with a geometrical area of ca. 0.2 cm^2 and a roughness factor of ca. 7.

product of NO_3^-, under constant electrolysis (vide infra), indicates that nitrite is formed. Note that the cyclic voltammograms shown in Figure 7A originate from a cross-linked de novo hemoprotein/NR assembly organized on a rough Au electrode[19] (roughness factor ca. 20−30). Figure 7A (inset) shows the electrocatalytic cathodic currents developed by the integrated de novo protein/NR electrode at different concentrations of nitrate. We see that the cathodic current levels off upon the increase of the nitrate concentration and reaches a saturation value at ca. $[NO_3^-] = 8.5 \times 10^{-2}$ M. As the observed cathodic current directly relates to the rate of the bioelectrocatalyzed reduction of NO_3^-, we analyzed the curve shown in Figure 7A (inset) in terms of the Michaelis−Menten model. Figure 7B shows the graphical Lineweaver−Burk analysis, eq 2, corresponding to the Michaelis−Menten kinetic model. This plot enables the extraction of the respective $I_{max} = 130$ μA and $K_M = 42$ mM values.

$$\frac{1}{I} = \frac{1}{I_{max}} + \frac{K_M}{I_{max}[NO_3^-]} \qquad (2)$$

To further characterize the kinetics of the electron-transfer rate within the complex formed between the substrate (NO_3^-) and the bioelectrocatalytic enzyme layer, we followed the electrocatalyzed reduction of NO_3^- using rotating-disk-electrode (RDE) experiments.[8d,33]

The electrocatalytic current, I_{cat}, is expected to be enhanced upon the increase of the rotating speed, due to the elimination of diffusional barriers for NO_3^- to the biocatalyst. Figure 8A, curve a, shows the Levich plot corresponding to the electrocatalytic current observed at different rotating speeds. Figure 8A, curve b, shows the theoretical Levich plot for the system, assuming only diffusional limitations for the electrocatalyzed reduction of NO_3^-. The experimental deviation of the Levich plot from linearity implies the existence of electron-transfer limitations in the electrocatalytic reduction of NO_3^-. Figure 8A (inset) shows the Koutecky−Levich plot (I_{cat}^{-1} vs $\omega^{-1/2}$) for the electrocatalytic currents at various rotating speeds. From this plot the heterogeneous electron-transfer rate constants, k_{et} (cm·s^{-1}) were evaluated using the different NO_3^- concentrations. The surface coverage of NR on the de novo protein layer was determined by complementary microgravimetric quartz-crystal-microbalance experiments, where the NR was cross-linked on a Au/quartz crystal modified with the de novo protein monolayer. Taking into account the surface coverage of NR, $\Gamma_{NR} \approx 2 \times 10^{-12}$ mol·cm^{-2}, the $k_{overall}$ values were extracted at different concentrations of NO_3^- (where $k_{overall} = k_{et}/\Gamma_{NR}$). Figure 8B shows the plot of the $k_{overall}^{-1}$ values at different NO_3^- concentrations. The fact that the plot does not reveal a constant value and exhibits a positive slope indicates the formation of a complex between NO_3^- and the bioelectrocatalytic interface,

(33) (a) Cenas, N. K.; Pocius, A. K.; Kulys, J. J. *Bioelectrochem. Bioenerg.* **1983**, *11*, 61. (b) Razumas, V. J.; Gudavicius, A. V.; Kulys, J. J. *J. Electroanal. Chem.* **1986**, *198*, 81.

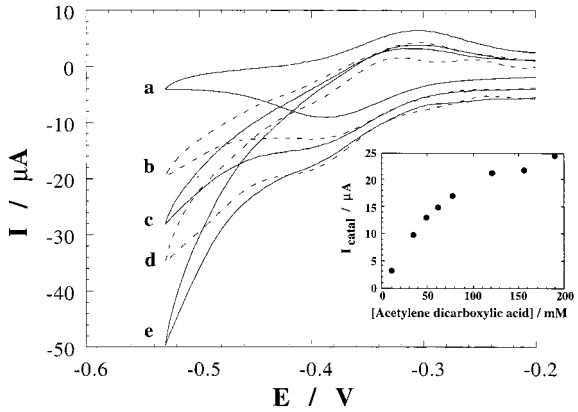

Figure 11. Cyclic voltammograms of the integrated Co(II)−myoglobin/Fe(III)−protoporphyrin IX-reconstituted de novo protein-layered Au electrode in the presence of different concentrations of acetylenedicarboxylic acid: (a) 0 mM, (b) 48 mM, (c) 78 mM, (d) 156 mM, and (e) 190 mM. Background electrolyte 0.1 M phosphate buffer, pH 7.0; under argon; potential scan rate 5 mV·s^{-1}; Au electrode roughness factor ca. 20, geometrical area ca. 2 cm^2. Inset: amperometric responses at $E = -0.52$ V at different concentrations of acetylenedicarboxylic acid.

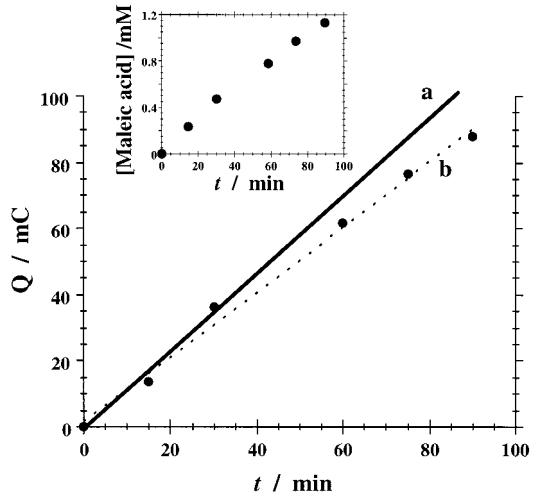

Figure 12. (a) Coulometric analysis of the charge passing through the electrolyte cell during hydrogenation of acetylenedicarboxylic acid (0.1 M) electrocatalyzed by the integrated Co(II)−myoglobin/Fe(III)−protoporphyrin IX-reconstituted de novo protein-layered Au electrode. (b) Calculated charge that passes the electrolyte cell according to the analyzed product, maleic acid. Background electrolyte 0.1 M phosphate buffer, pH 7.0; under argon; applied potential $E = -0.5$ V; Au electrode roughness factor ca. 20 and geometrical area ca. 2 cm^2. Inset: Concentration of electrogenerated maleic acid as a function of time.

Scheme 5. From the plot shown in Figure 8B the value for intracomplex electron transfer from NR to NO_3^-, $k_2 = 8.3 \times 10^4$ s^{-1}, was determined, and the value $K_M = 39$ mM was deduced, eq 3. The biocatalyzed reduction of nitrate by the

$$k_{overall} = k_2/(K_M + [NO_3^-]) \quad (3)$$

surface-modified electrode, assuming a Michaelis−Menten-type surface kinetics, was analyzed by the model developed by Lyons et al.[34] The derived values, $k_2 = 8.0 \times 10^4$ s^{-1} and $K_M = 35$ mM, are in good agreement to those derived by the Koutecky−Levich method.

The integrated de novo hemoprotein/NR monolayer−electrode was further examined in the constant-controlled-potential electrolysis of nitrate (NO_3^-), Figure 9. Samples of the electrolyte solution were analyzed at time intervals of electrolysis. Nitrite, NO_2^-, was identified as the only reduction product formed upon electrolysis. Figure 9, curve a, shows the charge passed through the cell during the electrolytic process. This curve is obtained upon the integration of the current passed over time. Figure 9, curve b, shows the calculated charge that should pass through the cell for the generation of the analyzed quantities of NO_2^- at the respective time intervals of electrolysis. (Note, these data assume a two-electron reduction of NO_3^- to NO_2^-). The current yield for the formation of NO_2^- is ca. 80%. The deviation from the theoretical value is attributed to oxygen leakage into the electrochemical cell during electrolysis.

Previous reports addressed the transformation of native hemoproteins to biocatalytic entities via the reconstitution of the apo-protein with metal−protoporphyrin IX substituents.[8b,c,10] Co(II)−porphyrins act as catalysts for the hydrogenation of acetylenes, presumably by the intermediate formation of a cobalt hydride species. For example, reconstitution of apo-myoglobin[10] or apo-α- or apo-β-hemoglobin[35] with Co(II)−protoporphyrin IX and secondary substitution of the respective proteins with a chromophore, e.g., eosin, was reported to yield photobioelectrocatalytic proteins for the hydrogenation of acetylenedicarboxylic acid to maleic acid. Thus, we tried to couple reconstituted native hemoproteins with the Fe(III)−protoporphyrin IX-reconstituted de novo protein monolayer−electrode. Apomyoglobin was reconstituted with Co(II)−protoporphyrin IX. The resulting Co(II)−protoporphyrin IX-reconstituted myoglobin, Co(II)−Mb, was interacted with the de novo protein monolayer−electrode. Figure 10 shows the cyclic voltammograms of the functionalized electrode in the absence of Co(II)−Mb, curve a, and in the presence of different concentrations of Co(II)−Mb, curves b−d. No electroreduction of Co(II)−Mb is observed at a bare Au electrode. These results clearly indicate that the functionalized monolayer associated with the electrode mediates electron transfer to Co(II)−Mb, presumably by the formation of an affinity complex between the two protein components.

To generate an integrated, electrically contacted biocatalytic electrode for the hydrogenation of acetylenes, the Fe(III)−protoporphyrin IX-reconstituted de novo protein monolayer−electrode was interacted with Co(II)−Mb to yield the layered affinity complex, Scheme 6. The latter assembly was then cross-linked with glutaric dialdehyde to generate the two-dimensional cross-linked Co(II)−Mb array onto the functionalized electrode. Figure 11 shows the cyclic voltammograms of the resulting de novo hemoprotein/Co(II)−Mb-layered electrode in the absence of acetylenedicarboxylic acid (**3**), curve a, and upon the addition of different concentrations of acetylenedicarboxylic acid (**3**), curves b−e.

In the presence of **3**, an electrocatalytic cathodic current is observed, indicating the electrocatalyzed reduction of **3**. The electrocatalytic current increases as the concentration of **3** is elevated, and it levels off to saturation at a concentration of **3** corresponding to 0.2 M, Figure 11 (inset). As the current response of the electrode relates to the rate of the electrocatalyzed reduction of **3**, the latter curve was analyzed in terms of the Michaelis−Menten model to yield $I_{max} = 40$ μA and $K_M = 80$ mM.

To identify the hydrogenation product of **3**, the electrically contacted integrated de novo hemoprotein/Co(II)−Mb was employed for the constant-potential electrolysis of **3** (−0.5 V),

(34) Lyons, M. E. G.; Lyons, C. H.; Michas, A.; Bartlett, P. N. *J. Electroanal. Chem.* **1993**, *351*, 245.

(35) Willner, I.; Zahavy, E.; Heleg-Shabtai, V. *J. Am. Chem. Soc.* **1995**, *117*, 542.

Scheme 7. Mechanism of the Hydrogenation of Acetylenedicarboxylic Acid Catalyzed by Co(II)−Myoglobin Electrically Contacted via Fe(III)−Protoporphyrin IX-Reconstituted de Novo Protein Monolayer

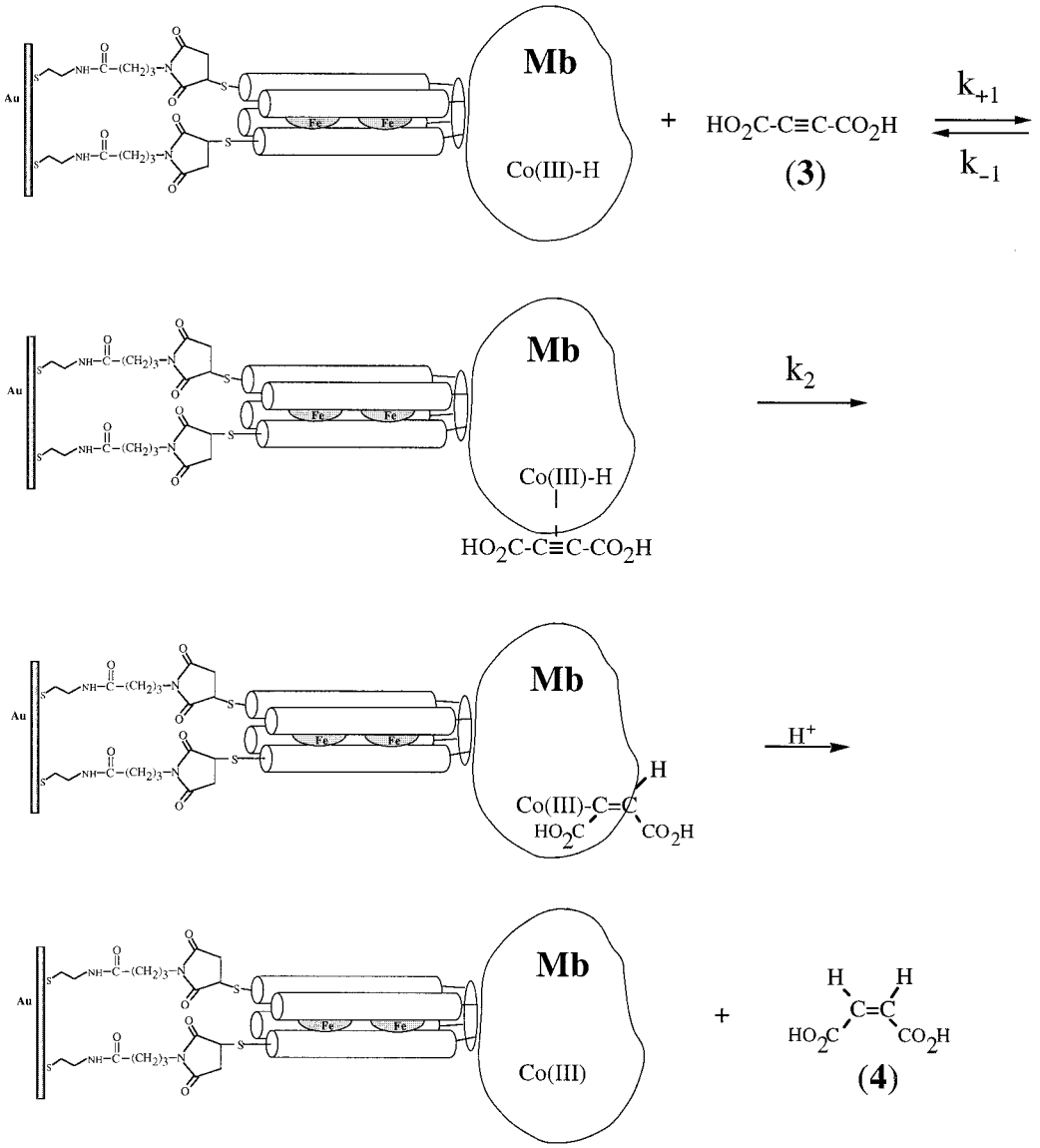

Figure 12. The electrolyte solution was analyzed at time intervals of electrolysis. The only reduction product that could be identified was maleic acid (**4**), and no fumaric acid could be identified. Figure 12, curve a, shows the charge passed through the electrochemical cell. This curve was obtained by the integration of the current over the time of electrolysis. Figure 12 (inset) shows the concentration of maleic acid (**4**) formed in the cell at time intervals of electrolysis. Figure 12, curve b, shows the calculated charge that is expected to pass through the cell to generate the analyzed quantities of maleic acid (**4**) (assuming that the transformation of **3** to **4** involves a two-electron process). The current yield for the formation of maleic acid is ca. 85%, and the deviation from the optimal current yield is attributed to O_2 leakage into the cell. It should be noted that no reduction potential of the C−C triple bond of acetylene compounds has been reported.[36] Spongy nickel, platinized platinum, palladized palladium, and silver-plated copper cathodes were used for the reduction of acetylenic compounds at extremely negative potentials corresponding to the electrolytic evaluation of hydrogen.[36,37] In a number of cases ethynes have been reduced to *cis*-olefins.[37a]

A possible pathway for the formation of maleic acid (**4**) was previously formulated[8b,c,10,35] and involves the formation of a cobalt hydride species that is the active intermediate in the hydrogenation of **3**, Scheme 7. Formation of the hydride species was supported by the observation of an isotope effect upon performing the hydrogenation in D_2O.[8c] According to this scheme, a complex between **3** and the electrogenerated Co(III)−H is formed, followed by the hydride transfer to the substrate, and formation of **4**. To support the formation of the complex between **3** and the de novo hemoprotein/Co(II)−Mb cross-linked assembly, and to elucidate the kinetics of intramolecular hydride transfer, the electrocatalytic hydrogenation of **3** was characterized by RDE experiments.

Figure 13A, curve a, shows the Levich plot corresponding to the electrocatalytic current resulting from the hydrogenation of **3** and the respective theoretical Levich plot, curve b. The deviation of I_{cat} from linearity as a function of $\omega^{1/2}$ implies that the electrocatalyzed hydrogenation of **3** is limited by electron transfer at high rotating speeds. Figure 13A (inset) shows the respective Koutecky−Levich plot from which the value k_{et}

(36) *Encyclopedia of Electrochemistry of the Elements;* Bard, A. J., Lund, H. Eds.; Marcel Dekker: New York, Organic Section, Vol. 11, pp 33−37.

(37) (a) Campbell, K. N.; Young, E. E. *J. Am. Chem. Soc.* **1943**, *65*, 965. (b) Beloslyudova, T. M.; Sokol'skii, D. B. *Elektrokhimiya* **1965**, *1*, 1182.

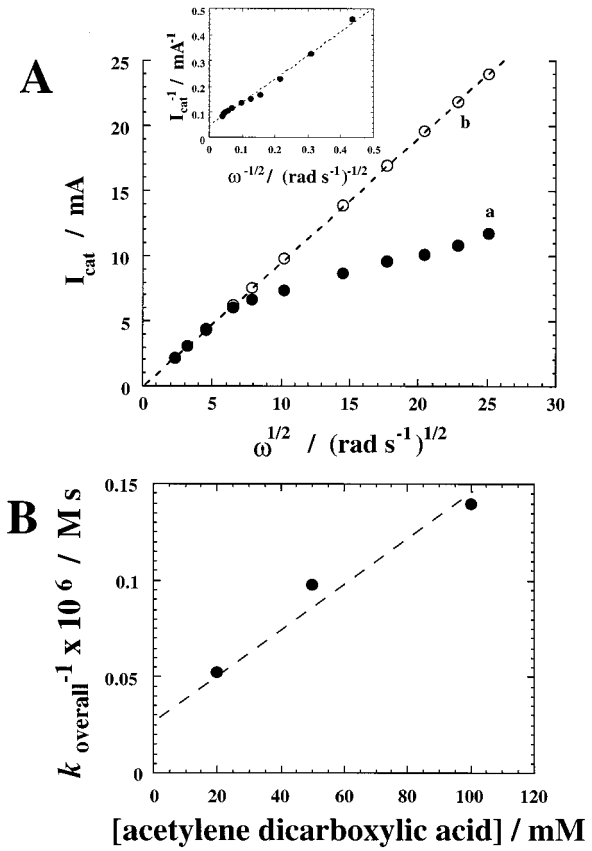

Figure 13. (A) Electrocatalytic currents corresponding to the hydrogenation of 50 mM acetylenedicarboxylic acid on the integrated Co(II)−myoglobin/Fe(III)−protoporphyrin IX-reconstituted de novo protein-layered Au rotating disk electrode vs $\omega^{1/2}$: (a) experimentally measured electrocatalytic currents at the applied potential $E = -0.5$ V; (b) theoretical Levich plot taking into account only diffusional limitations. Inset: Koutecky−Levich plot for the experimental electrocatalytic currents. Background electrolyte 0.1 M phosphate buffer, pH 7.0; under argon, Au disk electrode roughness factor ca. 1.3. (B) Second-order rate constants ($k_{overall}$) for the hydrogenation of acetylenedicarboxylic acid extracted from the RDE measurements.

(cm·s^{-1}) was evaluated, Figure 13B. By the determination of the different heterogeneous electron-transfer rate constants at different concentrations of **3**, and knowing the surface coverage of Co(II)−Mb on the bioelectrocatalytic interface, $\Gamma_{Co(II)-Mb} = 1 \times 10^{-12}$ mol·cm^{-2}, the respective $k_{overall}$ values at different concentrations of **3** were evaluated, Figure 13B. From this plot the values $k_2 = 8.2 \times 10^5$ s^{-1} and $K_M = 75$ mM were extracted. It should be noted that the surface coverage of Co(II)−Mb on the bioelectrocatalytic interface was determined by microgravimetric, QCM experiments, where the Co(II)−Mb was cross-linked on an Fe(III)−de novo protein monolayer associated with a Au/quartz crystal.

Conclusions

The present paper has addressed the assembly of a bifunctional Fe(III)−protoporphyrin de novo synthesized four-helix bundle protein monolayer−electrode on a Au electrode, and has discussed the use of the system for different bioelectronic applications. We have demonstrated that two Fe(III)−protoporphyrin IX units can be reconstituted into the de novo protein associated with the electrode support. The redox potentials of the Fe(III)−porphyrin sites reconstituted into the de novo protein are tuned and controlled by the intimate protein microenvironment. Similarly, the dynamics of the surface reconstitution of the four-helix bundle protein by the two Fe(III)−protoporphyrin IX sites is different, and the heme site exhibiting the more negative reduction potential enters slowly into the protein. Kinetic resolution and analysis of the interfacial reductive electron transfer to the bifunctional Fe(III)−protoporphyrin IX-reconstituted de novo protein reveal a fast single exponent electron transfer that was attributed to a rapid vectorial stepwise electron transfer in the assembly. The intramolecular vectorial electron transfer originates from the appropriate potential gradient in the structurally ordered heme assembly. Kinetic resolution of the interfacial oxidation of the reduced bifunctional de novo hemoprotein assembly revealed, however, a biexponential kinetics, originating from a potential barrier in the system that dictates a biphase, independent, electron transfer from the two heme sites in the four-helix bundle assembly to the electrode. The different interfacial electron-transfer kinetics for the reduction and oxidation of the de novo hemoprotein assembly enabled us to apply the functionalized electrode as a molecular rectifier exhibiting unidirectional electron-transfer properties.

The second aspect addressed in our paper relates to the surface engineering of electrodes with the cysteine-functionalized four-helix bundle protein. Direct immobilization of the protein into the Au electrode perturbs the tertiary structure of the de novo protein, presumably due to the nonspecific adsorption of amino acid residues. Covalent attachment of the four-helix bundle protein to monolayer matrixes of maleimide or *p*-hydroxymercury benzoate preserves the tertiary structure of the synthetic protein. The covalent coupling of proteins to the electrode by the *p*-hydroxymercury benzoate linker is of particular interest as it enables the regeneration of the surface with the active protein monolayer.

Finally, we discussed the use of the Fe(III)−protoporphyrin IX-reconstituted de novo protein as a synthetic cofactor for the electron-transfer activation of native redox proteins and semisynthetic reconstituted redox proteins. It has been demonstrated that by the surface cross-linking of affinity complexes formed between the de novo hemoprotein and nitrate reductase, NR, or Co(II)−protoporphyrin-reconstituted myoglobin, Co(II)−Mb, integrated, electrically contacted bioelectrocatalytic electrodes were assembled. The two-dimensional synthetic hemoprotein/NR layer assembly stimulated the bioelectrocatalyzed reduction of nitrate (NO_3^-) to nitrite (NO_2^-), and the potential application of the electrode as a nitrate sensor was discussed. The integrated synthetic hemoprotein/Co(II)−Mb-layered electrode was used for the electrocatalytic hydrogenation of acetylenedicarboxylic acid to maleic acid. The flexibility to tailor and tune the functions of de novo proteins opens a new methodology to structurally engineer novel macromolecular assemblies for bioelectronic applications.

Acknowledgment. This project is supported by the Deutsche Forschung sgemeinschaft (DFG), BMBF/Beo 22, and by the Volkswagen Stiftung, Germany.

JA983182U